

Piezoelectric Ribbons Printed onto Rubber for Flexible Energy Conversion

Yi Qi,[†] Noah T. Jafferis,[‡] Kenneth Lyons, Jr.,[†] Christine M. Lee,[†] Habib Ahmad,[§] and Michael C. McAlpine^{*·†}

[†]Department of Mechanical and Aerospace Engineering, Princeton University, [‡]Department of Electrical Engineering, Princeton University, Princeton, New Jersey 08544, and [§]Division of Chemistry and Chemical Engineering, California Institute of Technology, Pasadena, California 91125

ABSTRACT The development of a method for integrating highly efficient energy conversion materials onto stretchable, biocompatible rubbers could yield breakthroughs in implantable or wearable energy harvesting systems. Being electromechanically coupled, piezoelectric crystals represent a particularly interesting subset of smart materials that function as sensors/actuators, bioMEMS devices, and energy converters. Yet, the crystallization of these materials generally requires high temperatures for maximally efficient performance, rendering them incompatible with temperature-sensitive plastics and rubbers. Here, we overcome these limitations by presenting a scalable and parallel process for transferring crystalline piezoelectric nanothick ribbons of lead zirconate titanate from host substrates onto flexible rubbers over macroscopic areas. Fundamental characterization of the ribbons by piezo-force microscopy indicates that their electromechanical energy conversion metrics are among the highest reported on a flexible medium. The excellent performance of the piezo-ribbon assemblies coupled with stretchable, biocompatible rubber may enable a host of exciting avenues in fundamental research and novel applications.

KEYWORDS Energy conversion, piezoelectric nanoribbons, piezo force microscopy, flexible electronics, bioMEMS, nanomechanics

Efficient, highly portable energy sources have attracted increased interest due to the proliferation of hand-held consumer electronics. Decreasing power requirements for mobile electronics and nanodevices opens the possibility of augmenting batteries with systems that continuously scavenge otherwise wasted energy from the environment.¹ Most intriguing is the possibility of utilizing work produced by the human body via everyday activities, such as breathing or walking. For example, the heel strike during walking is a particularly rich source of energy with 67 W of power available from a brisk walker.² Harvesting even 1–5% of that power would be sufficient to run many body-worn devices such as mobile phones. Similarly, lung motion by breathing can generate up to 1 W of power.² If this power were harvested into charging a pacemaker battery, it may increase the time required between battery replacement surgeries for patients.

Smart materials contain properties that can be controllably altered by external stimuli. Of these, piezoelectric crystals are a particularly interesting subset that represent promising materials for electromechanical energy conversion technologies.^{3–8} These materials become electrically polarized when subjected to a mechanical stress, and conversely experience a strain in response to an applied electric field, and in proportion to the strength of the field.⁹ Single-crystal perovskites, such as lead zirconate titanate (PZT), are

an exceptionally efficient class of piezoelectric energy conversion materials. Indeed, PZT piezoelectric cantilevers operated near resonance have demonstrated mechanical to electrical energy conversion efficiencies above 80%.¹⁰

Epitaxial growth of such crystals depends on the use of rigid, inorganic host substrates, as well as high temperature deposition processes.¹¹ For example, rf-sputtering and metal-organic vapor deposition (MOCVD) at 600–700 °C have been shown to yield single-crystal films of PZT over large areas with excellent compositional control when deposited on MgO or SrTiO₃ substrates (lattice constants, *a*: PZT, 4.03–4.07 Å; SrTiO₃, 3.905 Å; MgO: 4.213 Å).^{12,13} Next-generation applications, such as wearable energy-harvesting systems, may require the piezoelectric materials to be flexible, lightweight, and biocompatible. The flexible piezoelectric polymer polyvinylidene difluoride (PVDF)¹⁴ has been used for applications such as shoe-sole power generators¹⁵ and implantable breath harvesting.¹⁶ However, these polymers suffer a number of drawbacks. The piezoelectric coefficient *d*₃₃ for PVDF (–26 pm/V)¹⁷ is an order of magnitude smaller than for inorganic lead zirconate titanate (PZT, >250 pm/V).¹⁸ PZT-PVDF composites can show high performance but rapidly degrade in air.¹⁹

The recently reported dry transfer process provides an efficient, robust approach for the relocation of semiconductor materials or fully fabricated devices from inorganic substrates to plastic using polydimethylsiloxane (PDMS) stamps or soluble glues.^{20–23} For example, we have recently shown that highly ordered semiconductor nanowire arrays can be comprehensively transferred from

* To whom correspondence should be addressed. Phone: (609) 542-0275. Fax: (609) 258-1918. E-mail: mcm@princeton.edu.

Received for review: 10/9/2009

Published on Web: 01/26/2010



their source wafers onto plastic substrates.^{22,24,25} The resulting flexible films demonstrated parts-per-billion (ppb) sensitivities to a host of small molecules when configured as chemical sensors.^{22,26}

Here, we present an approach to implementing crystalline piezoelectric PZT ribbons with micrometer-scale widths and nanometer scale thicknesses on rubber substrates over large areas for flexible energy conversion. First, PZT films were grown on a (100)-cleaved MgO crystal substrate and postannealed to form the perovskite crystal structure. Second, the structure, composition, and piezoelectric response of the films were characterized to ensure optimal performance. Next, the films were patterned into nanothick ribbons and printed onto PDMS via dry transfer. Finally, the fundamental piezoelectric properties were characterized on the rubber substrate using a nanoscale characterization method, piezoresponse force microscopy (PFM).²⁷

Figure 1 illustrates our printing process, which consists of the following key steps: (1) Preparation of crystalline PZT ribbons on MgO source wafers. Five hundred nanometers thick PZT was deposited using rf-sputtering from a $\text{Pb}(\text{Zr}_{0.52}\text{Ti}_{0.48})\text{O}_3$ target with 20% excess PbO onto an MgO substrate prepatterned with resist (AZ 1518, MicroChemicals). The resist was subsequently stripped via light sonication in acetone, and postannealing at 750 °C was performed to convert remaining PZT ribbons into the perovskite structure.²⁸ (2) Etching of the MgO wafer to free the PZT ribbons from their host. The MgO wafer with PZT ribbons was dipped in 20% phosphoric acid at 120 °C for 50 s. The exposed MgO between the PZT ribbons provides an avenue for the acid to undercut and loosen the ribbons without completely dislocating them. (3) Transfer printing of PZT ribbons by bringing a piece of PDMS (thickness ~2.5–5 mm) into conformal contact with the wafer and quickly peeling it back to retrieve the ordered ribbon arrays (Figure 1a). PZT ribbons were retrieved from the host substrate by the PDMS via noncovalent (van der Waals) forces, resulting in a flexible “piezo-rubber.”

Figure 1b shows, via optical microscopy, 500 nm thick, 5 μm wide PZT ribbons (10 μm center-to-center spacing) patterned on the host MgO substrate before transfer printing, and the ribbons following transfer to PDMS. It was found that the PZT ribbons were comprehensively transferred to the PDMS and remained uniform and continuous. A photograph of the resulting “piezo-rubber” chip (Figure 1c) confirms that the PZT ribbon array was cleanly and efficiently freed from the host wafer. In our experiment, over 95% of the ribbons were successfully transferred from MgO to PDMS over a 1 cm² area.

Obtaining high quality PZT thin films on inorganic host substrates is critical to ensuring optimal performance of PZT ribbons after transfer to PDMS. Studies have indicated an inherent reduction in the piezoelectric coefficient of thin PZT films due to internal defects.²⁹ Likewise, a stoichiometric composition near the morphotropic phase boundary of PZT

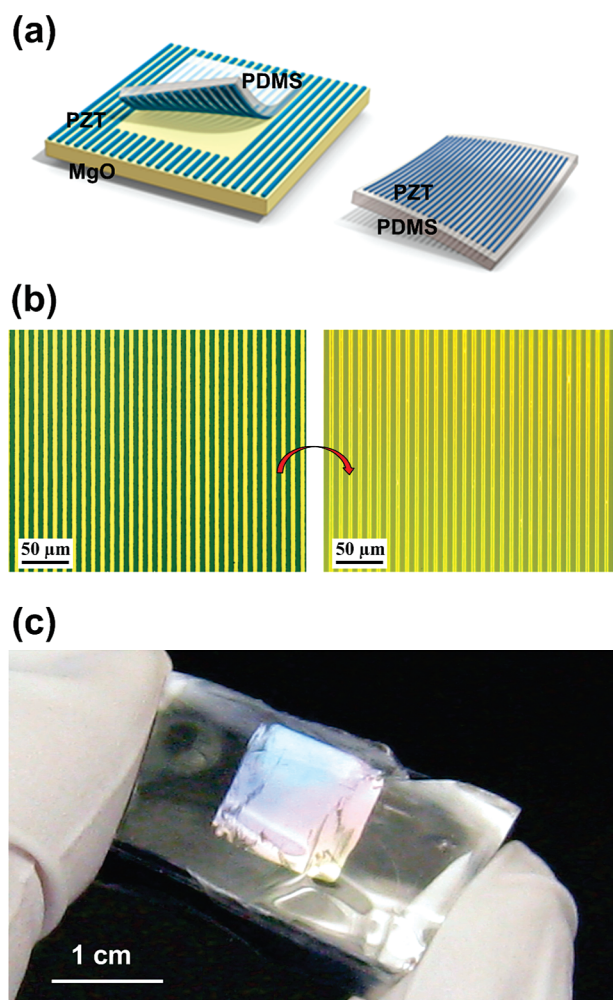


FIGURE 1. Transfer printing of PZT ribbons onto flexible rubber substrates. (a) Crystalline PZT ribbons are synthesized on an MgO host substrate, which is subsequently etched, and the ribbons are transfer printed onto flexible PDMS rubber. (b) Optical micrograph of PZT ribbons on MgO substrate before transfer, and PZT ribbons on PDMS after transfer printing. (c) Photograph of a piece of PDMS with PZT ribbons covering the top surface.

($\text{Pb}[\text{Zr}_x\text{Ti}_{1-x}]\text{O}_3$ with $x = 0.52$) is necessary for maximum piezoelectric response and poling efficiency. Thus, we performed rigorous compositional and structural characterization, as well as piezoelectric response measurements, on the PZT films from which the ribbons were patterned.

First, X-ray diffraction (XRD) and scanning electron microscopy (SEM) were used to characterize the structure of the PZT film (Figure 2a). The XRD data shows clear peaks corresponding to perovskite structure (100) and (200) faces, indicating a tendency toward epitaxial growth with a *c*-axis perpendicular to the film surface, while the perovskite (111) and pyrochlore peaks are relatively minor. Indeed, the SEM image shows no obvious surface texture. Energy dispersive spectroscopy (EDS) was then used to characterize the composition of the PZT film (Figure 2b). Comparison of the EDS curves for the annealed sample against a standard sample (52/48, Zr/Ti) shows peak intensities that were nearly identi-

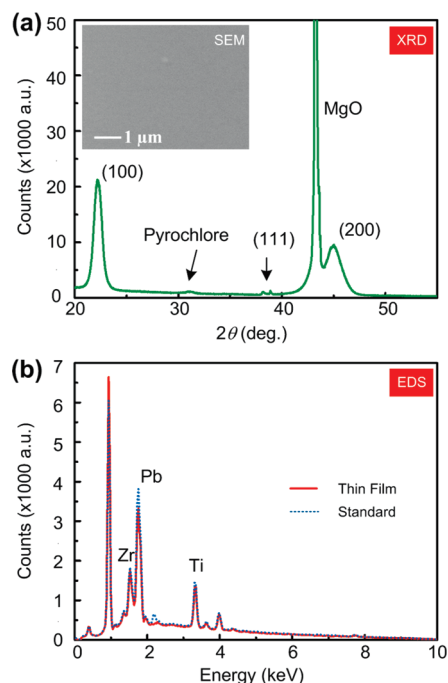


FIGURE 2. Thin-film PZT characterization. (a) XRD θ - 2θ scan of a PZT thin film prepared on MgO and heat-treated at 750 °C. Inset: SEM micrograph of the PZT film surface. (b) EDS curves of the annealed PZT thin film sample (red line) and a standard Zr/Ti 52/48 sample (blue dashed line).

cal for each element, indicating insignificant lead and zirconium loss during growth and postannealing.

Next, for characterizing the fundamental piezoelectric performance of the PZT film, the piezoelectric charge constants,³⁰ d_{ij} , were measured. Obtaining high d values is essential for energy harvesting applications, as the energy conversion efficiency (electromechanical coupling factor, k) of piezoelectrics scales proportionally with d . The most practical of the piezoelectric constants is d_{31} in the transverse operation mode. This mode has been used in applications such as energy generation from piezoelectric shoe implants.¹ Laser interferometers are the most established method for determining d_{31} in thin films,³¹ but require cantilever fabrication. An alternative for determining d_{31} is the “wafer flexure” approach.^{32,33} In this approach, a planar, two-dimensional mechanical stress is imposed on the PZT specimen via controlled bending by applying a uniform pressure (Figure 3a). Small deflection plate theory may then be used to determine the principal stresses, which are proportional to the applied pressure. Subsequently, the generated charge is collected across the 3-axis via a charge integrator circuit, and the ratio of the induced dielectric displacement to the applied stress determines d_{31} (see Supporting Information).

Figure 3b shows the results of our measurements, in which the charge density and pressure are oscillated in phase. The transverse piezoelectric constant, d_{31} was determined to be 49 pm/V for the as-annealed thin film sample. This spontaneous polarization of the film confirms the tendency of the c -axis of the film to be the out-of-plane

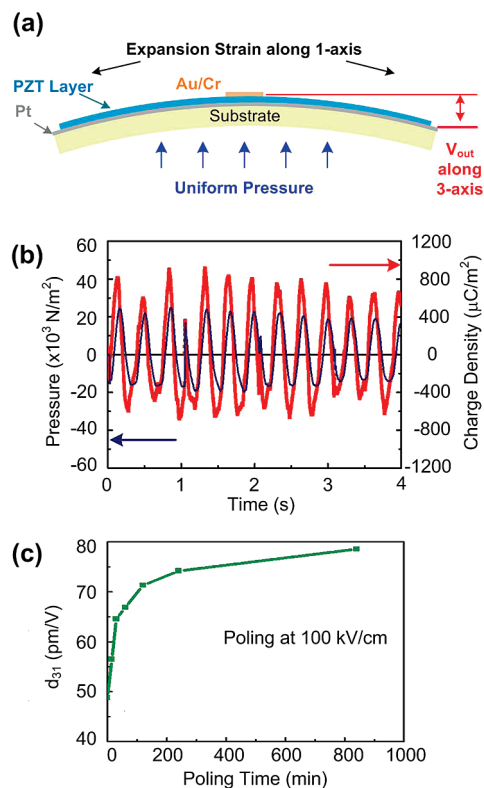


FIGURE 3. Transverse piezoelectric charge constant. (a) Schematic of a specimen indicating 31-mode piezoelectric bending and measurement. The PZT layer, top and bottom contact electrodes and substrate are indicated. (b) Oscillating pressure (left axis) and induced dielectric displacement (right axis). (c) d_{31} as a function of poling time at a poling field of ~ 100 kV/cm.

direction. Significantly, this value increased to $d_{31} = 79$ pm/V when the sample was poled at ~ 100 kV/cm for 14 h (Figure 3c). This value is in agreement with the best reported data for PZT films grown by sputtering³³ and is a factor of 3–4 times higher than typical values for PVDF ($d_{31, \text{PVDF}} = 20\text{--}25$ pm/V).³⁴

Particularly useful for characterizing our “piezo-rubber” is determining whether the piezoelectric performance is preserved after transfer of the PZT ribbons to PDMS. In this regard, the most critical indicator is the piezoelectric constant d_{33} , the induced polarization per unit stress applied in the out-of-plane (poling) direction. Piezoresponse force microscopy has become the accepted method for quantifying d_{33} where small displacements are involved.^{35,36} In PFM, an AC signal is first applied between a conducting atomic force microscope (AFM) tip and a bottom contact electrode. Next, the conducting tip is brought into contact with the surface. Finally, the electromechanical response of the surface is detected as optically mapped deflections of the tip. Thus, the tip simultaneously supplies current to the electrode and measures the inverse piezoelectric response.

To fully characterize the performance of our PZT ribbons, we conducted d_{33} measurements before and after transfer printing. The setup of the PFM measurement is illustrated in Figure 4a. A doped diamond conducting tip

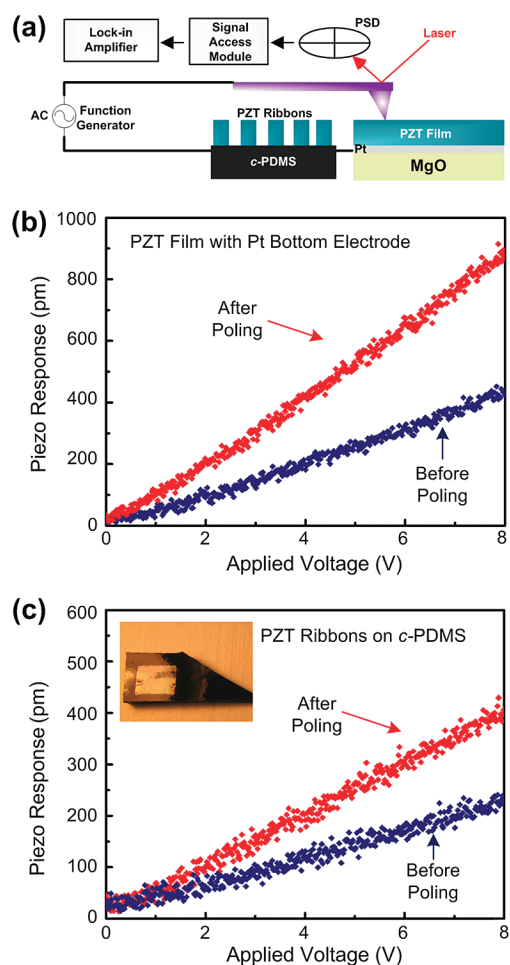


FIGURE 4. Piezoresponse force microscopy measurements. (a) Schematic of the PFM setup. An AC voltage is applied between the tip and bottom electrode, generating an oscillating strain that can be measured by the deflection signal using a lock-in amplifier. (b) Piezoresponse amplitude vs modulating AC bias voltage amplitude for PZT thin film. (c) Piezoresponse amplitude vs modulating AC bias voltage amplitude for PZT ribbons printed on *c*-PDMS. Inset: photograph of a slab of conducting PDMS (black) with PZT ribbons.

(radius 50 nm, Veeco DDESP-10) was used in contact mode, and an intermediate force applied (2000 nN) to ensure that the tip deflection is electromechanical response dominated.³⁵ An AC bias voltage of 40 kHz, chosen such that it was far away from the mechanical resonance frequency of the cantilever (320 kHz), was applied between the tip and the bottom electrode (Pt or conducting PDMS, as described below). The AC amplitude was ramped from 0 to 8 V (0 V DC bias) while the tip was held at one position. Finally, the slope of the piezoresponse amplitude (= vertical deflection \times sensitivity) versus modulation voltage amplitude was determined as the effective piezoelectric coefficient, d_{eff} . For the PZT film with an 80 nm Pt bottom electrode on MgO, the piezoelectric response amplitude was found to increase from 0 to 400 pm over the applied voltage range (Figure 4b), resulting in an effective piezoelectric coefficient of $d_{\text{eff}} = 57.0$ pm/V. The film was subsequently scanned with a 100

kV/cm bias voltage over a small area (100 nm²) for 60 min to pole the sample; d_{eff} was found to increase to 113.7 pm/V after poling. Control experiment on periodically poled lithium niobate (PPLN) crystals with known piezoelectric coefficients suggested a good agreement between d_{eff} and d_{33} for our experimental conditions (see Supporting Information). This thin film value is also comparable to values for MOCVD-deposited PZT films.³⁷

Most significantly, we performed d_{eff} measurements on PZT ribbons after transfer to PDMS. The PDMS was rendered conducting by adding 13 wt % fine carbon black (Vulcan XC72; Cabot, Billerica, MA) to the prepolymer before curing.³⁸ The PFM conditions were altered such that the applied force was 500 nN to avoid delaminating the ribbons from the PDMS surface. Figure 4c shows the piezoelectric response versus modulation voltage measured on PZT ribbons stamped onto this conducting PDMS (*c*-PDMS), which serves as bottom electrode. For the as-transferred sample, d_{eff} was found to be 27.1 pm/V, while with poling was found to yield $d_{\text{eff}} = 50.5$ pm/V. The combination of a large tip radius and small force for these experiments suggests operation in the weak-indentation regime for which an estimated conversion factor $d_{\text{eff}} = 0.5 d_{33}$ should be applied.³⁵ This results in d_{33} values of 54.2 and 101.0 pm/V for PZT ribbons before and after poling, respectively. These values agree well with the thin film data, which is understandable considering the relatively benign processing conditions for fabricating and transferring PZT ribbons. In particular, the value of $d_{33} = 101.0$ pm/V for PZT ribbons on PDMS represents a 4-fold improvement over similar values for ZnO nanobelts on rigid substrates ($d_{33, \text{ZnO nanobelt}} = 27$ pm/V)³⁶ for flexible PVDF polymers ($d_{33, \text{PVDF}} = -26$ pm/V)¹⁷ and for PZT-PVDF hybrid composites ($d_{33} = 15-25$ pm/V).³⁹

In summary, highly crystalline piezoelectric ceramic ribbons have been transferred in high yields and over large areas onto rubber substrates. These flexible piezo-assemblies have been shown to be particularly efficient electromechanical energy converters, representing a promising step toward the implementation of wearable or even implantable energy harvesters, and biological force sensing microdevices. Yet, a number of key challenges remain. In particular, future work will help us understand in more detail (1) the mechanics of the piezoelectric on a stretchable platform, (2) the hard inorganic/soft polymeric interface and its longevity under mechano-electrical cycling, and (3) the cointegration of power rectification and regulation electronics on the flexible support.

Acknowledgment. We thank N. Yao and G. Poirier for useful discussions. M.C.M. acknowledges primary support of this work via the Young Investigator Award from the Intelligence Community (No. 2008*1218103*000).

Supporting Information Available. Details about the experimental setup for measuring the transverse piezoelectric constant, d_{31} , as well as calibration experiments for PFM

using a PPLN standard sample. This material is available free of charge via the Internet at <http://pubs.acs.org>.

REFERENCES AND NOTES

- (1) Paradiso, J. A.; Starner, T. *IEEE Pervas. Comput.* **2005**, *4*, 18–27.
- (2) Starner, T. *IBM Syst. J.* **1996**, *35*, 618–629.
- (3) Priya, S.; Inman, D. J. *Energy Harvesting Technologies*; Springer: New York, 2008.
- (4) Yang, R.; Qin, Y.; Dai, L.; Wang, Z. L. *Nat. Nanotechnol.* **2009**, *4*, 34–39.
- (5) Yang, R.; Qin, Y.; Li, C.; Zhu, G.; Wang, Z. L. *Nano Lett.* **2009**, *9*, 1201–1205.
- (6) Serrell, D.; Law, J.; Slifka, A.; Mahajan, R.; Finch, D. *Biomed. Microdevices* **2008**, *10*, 883–889.
- (7) Srinivasan, S.; Hiller, J.; Kabiuss, B.; Auciello, O. *Appl. Phys. Lett.* **2007**, *90*, 134101.
- (8) Muralt, P.; Polcawich, R. G.; Trolrier-McKinstry, S. *MRS Bull.* **2009**, *34*, 658–664.
- (9) Jaffe, H. J. *Am. Ceram. Soc.* **1958**, *41*, 494–498.
- (10) Flynn, A. M.; Sanders, S. R. *IEEE Trans. Power Electron.* **2002**, *17*, 8–14.
- (11) Kingon, A. I.; Srinivasan, S. *Nat. Mater.* **2005**, *4*, 233–237.
- (12) Takayama, R.; Tomita, Y. *J. Appl. Phys.* **1989**, *65*, 1666–1670.
- (13) Foster, C. M.; Bai, G.-R.; Csencsits, R.; Vetrone, J.; Jammy, R.; Wills, L. A.; Carr, E.; Amano, J. J. *Appl. Phys.* **1997**, *81*, 2349–2357.
- (14) Vinogradov, A.; Holloway, F. *Ferroelectrics* **1999**, *226*, 169–181.
- (15) Shenck, N. S.; Paradiso, J. A. *IEEE Micro* **2001**, *21*, 30–42.
- (16) Hausler, E.; Stein, L.; Harbauer, G. *Ferroelectrics* **1984**, *60*, 277–282.
- (17) Furukawa, T.; Seo, N. *Jpn. J. Appl. Phys.* **1990**, *29*, 675–680.
- (18) Li, J.-F.; Dai, X.; Chow, A.; Viehland, D. *J. Mater. Res.* **1995**, *10*, 926–938.
- (19) Chen, X. D.; Yang, D. B.; Jiang, Y. D.; Wu, Z. M.; Li, D.; Gou, F. J.; Yang, J. D. *Sens. Actuators, A* **1998**, *65*, 194–196.
- (20) Ahn, J.-H.; Kim, H.-S.; Lee, K. J.; Jeon, S.; Kang, S. J.; Sun, Y.; Nuzzo, R. G.; Rogers, J. A. *Science* **2006**, *314*, 1754–1757.
- (21) Javey, A.; Nam, S.-W.; Friedman, R. S.; Yan, H.; Lieber, C. M. *Nano Lett.* **2007**, *7*, 773–777.
- (22) McAlpine, M. C.; Ahmad, H.; Wang, D.; Heath, J. R. *Nat. Mater.* **2007**, *6*, 379–384.
- (23) Fan, Z. Y.; Ho, J. C.; Jacobson, Z. A.; Yerushalmi, R.; Alley, R. L.; Razavi, H.; Javey, A. *Nano Lett.* **2008**, *8*, 20–25.
- (24) Friedman, R. S.; McAlpine, M. C.; Ricketts, D. S.; Ham, D.; Lieber, C. M. *Nature* **2005**, *434*, 1085.
- (25) McAlpine, M. C.; Friedman, R. S.; Lieber, C. M. *Proc. IEEE* **2005**, *93*, 1357–1363.
- (26) McAlpine, M. C.; Agnew, H. D.; Rohde, R. D.; Blanco, M.; Ahmad, H.; Stuparu, A. D.; Goddard, W. A.; Heath, J. R. *J. Am. Chem. Soc.* **2008**, *130*, 9583–9589.
- (27) Bonnell, D. A.; Kalinin, S. V.; Kholkin, A. L.; Gruverman, A. *MRS Bull.* **2009**, *34*, 648–657.
- (28) Zhang, X. Y.; Zhao, X.; Lai, C. W.; Wang, J.; Tang, X. G.; Dai, J. Y. *Appl. Phys. Lett.* **2004**, *85*, 4190–4192.
- (29) Dunn, S. *Integr. Ferroelectr.* **2003**, *59*, 1505–1512.
- (30) *IEEE/ANSI 176 IEEE Standard on Piezoelectricity*; The Institute of Electrical and Electronics Engineers (IEEE), Inc.: New York, 1987.
- (31) Kholkin, A. L.; Wutchrich, C.; Taylor, D. V.; Setter, N. *Rev. Sci. Instrum.* **1996**, *67*, 1935–1941.
- (32) Shepard, J. J. F.; Moses, P. J.; Trolrier-McKinstry, S. *Sens. Actuators, A* **1998**, *71*, 133–138.
- (33) Shepard, J. F.; Chu, F.; Kanno, I.; Trolrier-McKinstry, S. *J. Appl. Phys.* **1999**, *85*, 6711–6716.
- (34) In *Polymeric Materials Encyclopedia*; Salamone, J. C., Ed.; CRC Press: Boca Raton, 1996; Vol. 9.
- (35) Kalinin, S. V.; Bonnell, D. A. *Phys. Rev. B* **2002**, *65*, 125408–125418.
- (36) Zhao, M.-H.; Wang, Z.-L.; Mao, S. X. *Nano Lett.* **2004**, *4*, 587–590.
- (37) Lefki, K.; Dormans, G. J. M. *J. Appl. Phys.* **1994**, *76*, 1764–1767.
- (38) Unger, M. A.; Chou, H. P.; Thorsen, T.; Scherer, A.; Quake, S. R. *Science* **2000**, *288*, 113–116.
- (39) Venkatragavaraj, E.; Satish, B.; Vinod, P. R.; Vijaya, M. S. *J. Phys. D: Appl. Phys.* **2001**, *34*, 487–492.